nature energy

PERSPECTIVE

https://doi.org/10.1038/s41560-020-0674-x

Check for updates

Realizing high zinc reversibility in rechargeable batteries

Lin Ma[1], Marshall A. Schroeder[1]✉, Oleg Borodin[1], Travis P. Pollard[1], Michael S. Ding[1], Chunsheng Wang[2] and Kang Xu[1]✉

Rechargeable zinc metal batteries (RZMBs) offer a compelling complement to existing lithium ion and emerging lithium metal batteries for meeting the increasing energy storage demands of the future. Multiple recent reports have suggested that optimized electrolytes resolve a century-old challenge for RZMBs by achieving extremely reversible zinc plating/stripping with Coulombic efficiencies (CEs) approaching 100%. However, the disparity among published testing methods and conditions severely convolutes electrolyte performance comparisons. The lack of rigorous and standardized protocols is rapidly becoming an impediment to ongoing research and commercialization thrusts. This Perspective examines recent efforts to improve the reversibility of the zinc metal anode in terms of key parameters, including CE protocols, plating morphology, dendrite formation and long-term stability. Then we suggest the most appropriate standard protocols for future CE determination. Finally, we envision future strategies to improve zinc/electrolyte stability so that research efforts can be better aligned towards realistic performance targets for RZMB commercialization.

The rapidly growing markets of electric vehicles, mobile electronics and grid storage have driven annual lithium-ion battery (LIB) production to >150 GWh yr^{-1} (ref. [1]). However, in light of high cost, known safety issues and potential resource concerns, both geopolitically and ethically, over the mining of lithium, graphite and cobalt[2,3], the development of alternative energy storage solutions complementary to LIBs has become increasingly urgent. A rechargeable zinc metal battery (RZMB) can address these needs due to zinc's compatibility with non-flammable aqueous electrolytes[4–8], approximately threefold higher volumetric capacity[9] (5,854 Ah l^{-1}), high gravimetric capacity (820 mAh g^{-1}) and much higher abundance in Earth's crust when compared with Li[10]. Success has been achieved in cathode materials for RZMBs, including various metal oxides (for example, MnO_2 (ref. [11]), $Zn_{0.25}V_2O_5{\cdot}nH_2O$ (ref. [4]), Bi_2O_3 (ref. [12]) and so on), layered sulfides[13], Prussian blue analogues[14] and organic materials[15]. However, several key scientific issues surrounding the Zn metal electrode still impede RZMB commercialization, including poor Coulombic efficiency (CE), large voltage polarization, and a propensity for dendritic failure, each of which has plagued Zn reversibility for centuries dating back to Alessandro Volta's Cu/Zn piles.

Each of these challenges stem directly or indirectly from the interaction between Zn metal and the electrolytes. Hence, extensive efforts in recent years have focused on tailoring new aqueous[6–8,16–19] and non-aqueous[14,20–24] electrolytes, many of which are published with extremely encouraging CE values for Zn plating/stripping: 99.90% for 1 m zinc bis(trifluoromethylsulfonyl)imide ($Zn(TFSI)_2$) + 20 m lithium bis(trifluoromethylsulfonyl)imide (LiTFSI)[6] in H_2O; 99.68% for 0.5 M zinc trifluoromethanesulfonate ($Zn(OTf)_2$) in triethyl phosphate[14]; 100% for 1 M $Zn(OTf)_2$ in H_2O (ref. [19]); and 100% for 0.5 M $Zn(TFSI)_2$ in propylene carbonate[22]. However, despite multiple claims of 100% CE (a perfectly reversible system with unlimited cycles to failure), a commercial RZMB does not yet exist. This disconnect can be traced back to disparities between CE testing protocols and realistic RZMB requirements. The absence of a standard CE determination protocol under uniform conditions precludes effective comparisons across electrolyte systems. This not only creates public confusion in accurately assessing the technology status but also, more importantly, it prevents researchers from developing and evaluating new materials and obscures funding managers from allocating resources to the most promising systems.

In this Perspective, we examine current efforts to quantify the reversibility of Zn metal plating/stripping, which critically depends on the electrolytes and interphasial chemistries. Analogous to a recent Perspective on lithium metal[25], we classify published efforts according to four key test parameters: areal current density, areal capacity per cycle, cumulative capacity of Zn plated and the associated CEs. Using these metrics, we compare current approaches against the proposed commercial targets for the Zn metal anode in RZMBs. We expose the disadvantages of cyclic voltammetry (CV), which has been frequently used as a method to determine the CE, and suggest two types of established galvanostatic protocol as the standard.

Current state of Zn reversibility

Figure 1 summarizes the published CE values for Zn plating/stripping in various aqueous and non-aqueous electrolytes obtained from a variety of test protocols and cell setups, with a detailed breakdown of each data point in Supplementary Table 1. We compare these CEs according to three testing parameters: the cumulative capacity of Zn plated before cell shorting or excessive impedance generation, which is a critical indicator of cell lifetime; the plating/stripping current density; and the areal capacity of Zn plated during each cycle.

There are three surprising takeaways from Fig. 1. First, more than half of the currently published Zn electrolytes in the literature claim CEs >99%. Second, the parameters selected for these CE measurements are highly scattered and appear arbitrary, rather

[1]Energy Storage Branch, Energy and Biotechnology Division, Sensor and Electron Devices Directorate, US Army Research Laboratory, Adelphi, MD, USA. [2]Department of Chemical and Biomolecular Engineering, University of Maryland, College Park, MD, USA. ✉e-mail: marshall.a.schroeder.civ@mail.mil; conrad.k.xu.civ@mail.mil

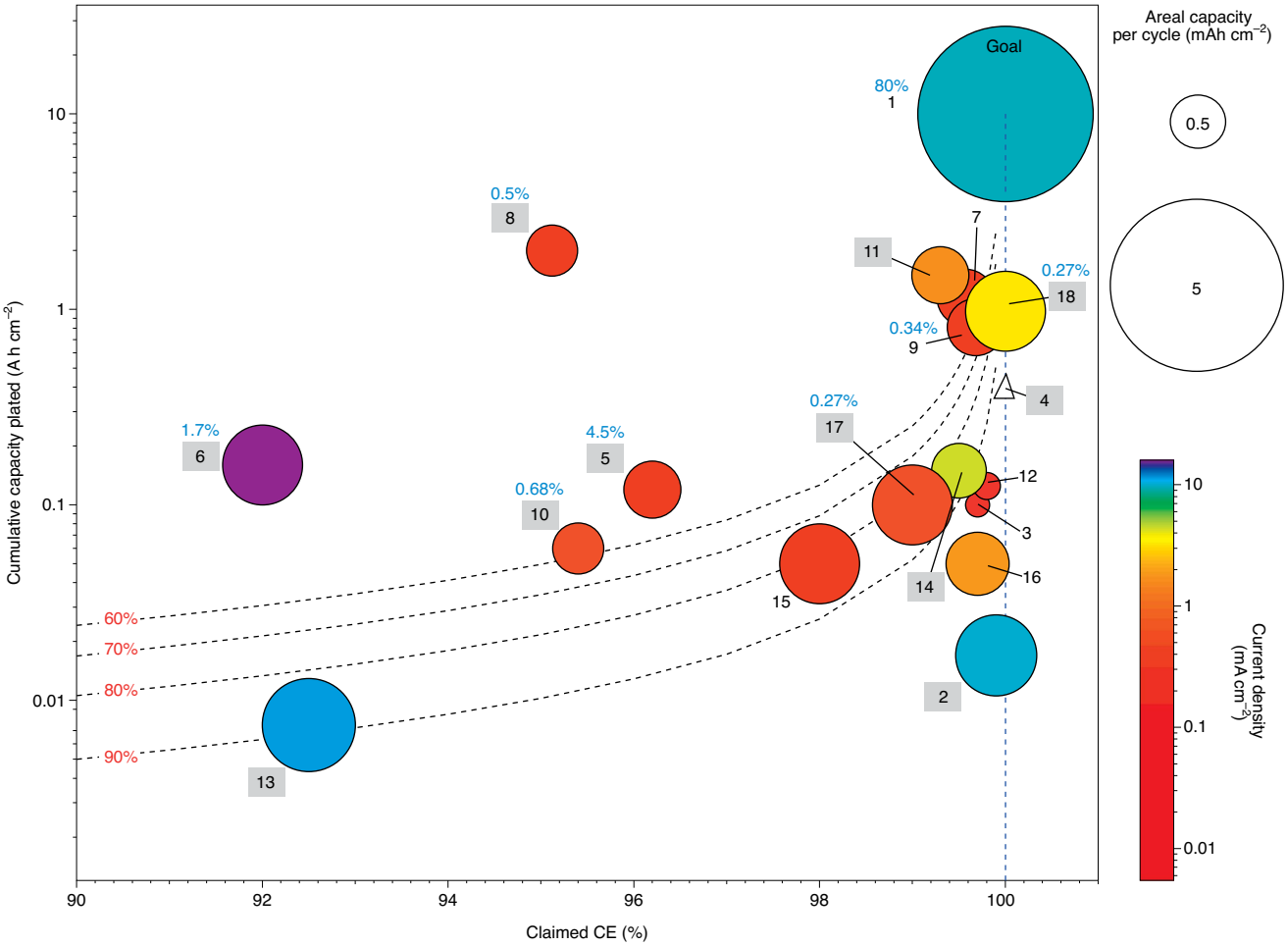

Fig. 1 | Summary of published Zn plating/stripping CE measurements. The published data are analysed in terms of three parameters: cumulative areal capacity plated (*y* axis), per-cycle areal capacity (diameter) and plating current density (heatmap). Point 1[25,26] represents a competitive commercial RZMB target (5 mAh cm^{-2}, 80% Zn utilization and 2C charging rate). Point 4[19] is denoted with a triangle as the areal capacity plated per cycle and current density were not reported. The contour dashed lines represent the relationship between cumulative capacity plated (before capacity retention reaches 60%, 70%, 80% and 90%, respectively) and CE estimated using the parameters of point 1 without considering the effect dendrite formation, where the vertical dashed line represents the ideal case of infinite cycle life that can only be approached indefinitely. Numbers in grey squares represent aqueous electrolyte efforts. The utilization of Zn per cycle is labelled in blue text, where available. Points 2 (ref. [6]), 3 (ref. [23]), 4 (ref. [19]), 13 (ref. [17]), 14 (ref. [17]) and 16 (ref. [24]) were obtained using the CV method and points 5–12 (refs. [7,8,14,16,18,20,21,38]), 15 (ref. [24]), 17 (ref. [34]) and 18 (ref. [34]) were obtained by the galvanostatic method. See Supplementary Table 1 for the reference, description and values for each point.

than aligning towards a rigorous protocol linked to performance in a practical RZMB. Finally, most of the published CEs correspond to only a small fraction of Zn utilized per cycle, typically less than 1%, which is impractically low for commercial viability. The latter two naturally cast doubt over the optimism delivered by the first. This conflict reflects the relative immaturity of the RZMB chemistry compared with LIBs and lithium metal batteries (LMBs), so it is evident that the field must establish a consensus regarding performance targets for commercial viability of RZMBs, as researchers did for LIBs and LMBs.

To this end, a commercial target with an ideal CE of 100% and at least 2,000 cycles (cumulative plated capacity of 10 A h cm^{-2}) was set as point 1 in Fig. 1, and represents the goal for an LMB with a loading of 5 mAh cm^{-2} with 80% of the Li passed per cycle that is also capable of a fast charging rate of 2C, or 10 mA cm^{-2} (refs. [25,26]). Applying this target to the current progress in Zn, it is clear that improvements of at least one order of magnitude are needed in plating/stripping current density, the corresponding areal capacity and Zn utilization (or depth of discharge, DOD) per cycle to approach a competitive RZMB. Contour lines are also created in Fig. 1 to illustrate the relationship between CE and the Zn metal electrode cycle lifetime, which corresponds to the cumulative capacity plated before reaching a certain capacity retention (%). Using a CE of 99% with parameters corresponding to point 1 as an example, a Zn metal electrode would only last ~22 cycles (that is, plated ~110 mAh cm^{-2}) before its capacity retention dropping to 80%, if dendritic failure does not occur earlier than the 22nd cycle. The CE must be improved to 99.97% if the same capacity retention is required at the 1,000th cycle[25].

Unsettling CE measurements

The techniques and control parameters selected for quantifying CE merit special discussion. Two common electrochemical techniques are often adopted in determining Zn plating/stripping CE. The first is potentiodynamic cycling, as represented by CV, in which the working electrode potential is swept at a constant rate (mV s^{-1}) within a potential window that encompasses Zn deposition and stripping. The other is galvanostatic cycling, in which plating/stripping

is conducted at a fixed current density until reaching a certain capacity and/or cut-off potential[27]. In principle, both experiments measure the reversibility of the system by comparing the amount of Zn plated with the amount of Zn recovered thereafter, but they operate under very different conditions and result in distinctly different physical and chemical states of the working electrode.

In CV, the user-defined conditions include potential scan rate (mV s^{-1}), potential range (versus either a reference or a Zn counter/reference electrode) and working electrode substrate (copper, platinum and so on). However, multiple conditions relevant to battery performance, such as plating/stripping current density or the cycled areal capacity, cannot be controlled in CV. In addition, the working electrode in CV experiences a much different electrochemical environment from that in a battery, in which the Zn metal anode is situated very close to the Zn/Zn^{2+} potential instead of sweeping around it at a constant rate to the potentials selected for the experiment. To draw meaningful performance comparisons across systems and methods in Fig. 1, the plating current density and areal capacity per cycle of the points measured by CV were estimated using average current, but it is immediately clear that these values are too scattered (Fig. 1) to allow any meaningful comparison, even within the same experimental setup. In some CV measurements, the surface area of Zn electrode immersed in the electrolyte is also difficult to determine or is not explicitly stated; thus, the current density and areal capacity cannot be calculated accurately (for example, point 4 in Fig. 1).

Figure 2a shows selected digitized CV curves for several state-of-the-art electrolytes[6,19,22–24]. The reported current or current density is normalized here to allow a clear comparison of the potential range. Theoretically, the potential range during a CV scan is divided into two parts: the plating window (<0 V versus Zn/Zn^{2+}) and the stripping window (>0 V versus Zn/Zn^{2+}), in which the amount of plated and stripped Zn can be calculated, respectively. However, in a real battery, the Zn stripping potential is subject to restrictions imposed by the cathode chemistry, the current density and the full-cell discharge cut-off voltage. The Zn plating potential is also required to be as close to 0 V (versus Zn/Zn^{2+}) as possible (ideally within −0.1 V for most aqueous electrolytes) to reduce the charge voltage and minimize electrolyte decomposition via hydrogen evolution or reduction reactions. With carefully selected parameters, a CV scan can be designed to operate within the Zn plating and stripping potentials of a real cell.

In reality, many published works selected rather unrealistic potential ranges for plating (Fig. 2a), with some even beyond −0.5 V versus Zn/Zn^{2+}. This extremely large overpotential for Zn deposition would generally not be accessible in a full cell. Many of the published CV studies also include unrealistically high cut-off stripping potentials, with some even beyond the operating potentials of common Zn cathode materials, as shown in the floating bars in Fig. 2a. To put this in perspective, if this condition occurred in an actual cell, the full-cell voltage would be negative at the end of discharge. The underlying motivation for adopting those unrealistic upper potentials is the inability to either plate or recover the plated Zn within a realistic potential window, usually due to high polarization caused by either high interfacial impedance or poor electrolyte conductivity.

Here, to compare published results with those achievable in a full cell, we extracted CE values at an upper stripping potential of 0.2 V (the lowest discharge cut-off voltage among the listed full-cell chemistries) and 0.5 V, respectively, for all the CV curves. The former leads to a stark reduction in the achievable CEs from the otherwise nearly 100% values. On the basis of these considerations and the dependence of these results on user-defined conditions not relevant to battery operation, we strongly discourage CV as a method for CE studies.

Establishing a standard protocol

The alternative to CV is the galvanostatic technique[7,8,14,18,21,24]. This method provides more direct control over those parameters relevant to battery operation (areal capacity, current density and voltage window); however, major variability still exists in published test parameters and setups.

Here we recommend a 'reservoir half-cell' method (Fig. 2b), initially introduced by Aurbach et al. and subsequently adopted by others[28–30], as a standard template so that these key factors affecting Zn reversibility can be evaluated. Using a Zn|(selected metal substrate) cell setup, this protocol calls for an initial conditioning cycle in which a certain areal capacity of Zn is plated and then stripped from the metal substrate working electrode. This conditioning step diminishes substrate effects (for example, lattice mismatch, alloying, interphase effects and so on). A reservoir of Zn with specific areal capacity (Q_r) is then plated on the metal substrate to provide a limited and well-controlled source of Zn for subsequent CE determination. A fraction of this Zn reservoir is then cycled several times (n) at a fixed capacity (Q_c) using a specific current density, followed by stripping to a preselected upper cut-off voltage, which indicates all removable Zn (Q_s) has been stripped, including the initial reservoir. The average CE can be calculated according to the equation shown in Fig. 2b.

To align with published efforts, we recommend a standard areal current density (0.5 mA cm^{-2}), areal capacity (1 mAh cm^{-2}) and upper cut-off voltage (0.5 V versus Zn/Zn^{2+}) as an initial screening experiment. The number of cycles should be modest enough (for example, ten) to avoid interference from dendrite formation or excessive impedance growth. In addition, a Q_c/Q_r ratio of 1/5 with a 100-μm-thick Zn foil counterelectrode is also recommended for the purpose of normalization.

Three factors provide the basis for these specific screening parameters. First, they are the most commonly published galvanostatic cycling parameters, meaning that they will provide a useful benchmark between previously published and future studies; second, the parameters are reasonably achievable for both aqueous and non-aqueous systems; and finally the parameters are a reasonable step towards the proposed commercial targets (point 1 in Fig. 1), which no electrolyte can currently achieve, yet still rigorous enough that the least efficient electrolytes are not able to pass the protocol and hence eliminated early enough from further study.

As a validation, application of this standardized method has already been demonstrated to effectively rank Zn plating/stripping CEs among different aqueous and non-aqueous electrolytes[7,8,29]. For the most promising systems with extremely high CE values (>99%), an even more rigorous 'reservoir free' galvanostatic protocol in the configuration of Zn|(metal substrate) or Zn|cathode with an ultrathin (for example, ≤30 μm (ref. [25])) Zn metal anode (Fig. 2c) can be subsequently applied. Electrolytes that can pass this protocol would gain high confidence in being capable of supporting higher-energy-density cell formats.

Effects from morphology, utilization and rate

Zn reversibility in an actual battery environment also depends on other factors than CE, the most important are perhaps the morphology in which Zn is plated and the fraction of Zn plated from the Zn electrode (or DOD). In this sense, a 100% CE is not necessarily indicative of a promising Zn system. Thus, tracking the relation between the CE and these properties could potentially guide performance improvements.

Unlike LMBs, in which dendrite formation is promoted by high plating currents in both liquid and solid electrolytes, an inverse behaviour has been reported for aqueous zinc sulfate ($ZnSO_4$) electrolytes. Scanning electron microscope (SEM) images reveal that at low current density (Fig. 3c–e), the deposited Zn is highly porous and consists of thin flakes that penetrate the separator and cause battery failure (Fig. 3a). Surprisingly, dense Zn deposition was observed at a current density increased by an order of magnitude (Fig. 3f,g) at the same areal capacity (1 mAh cm^{-2}).

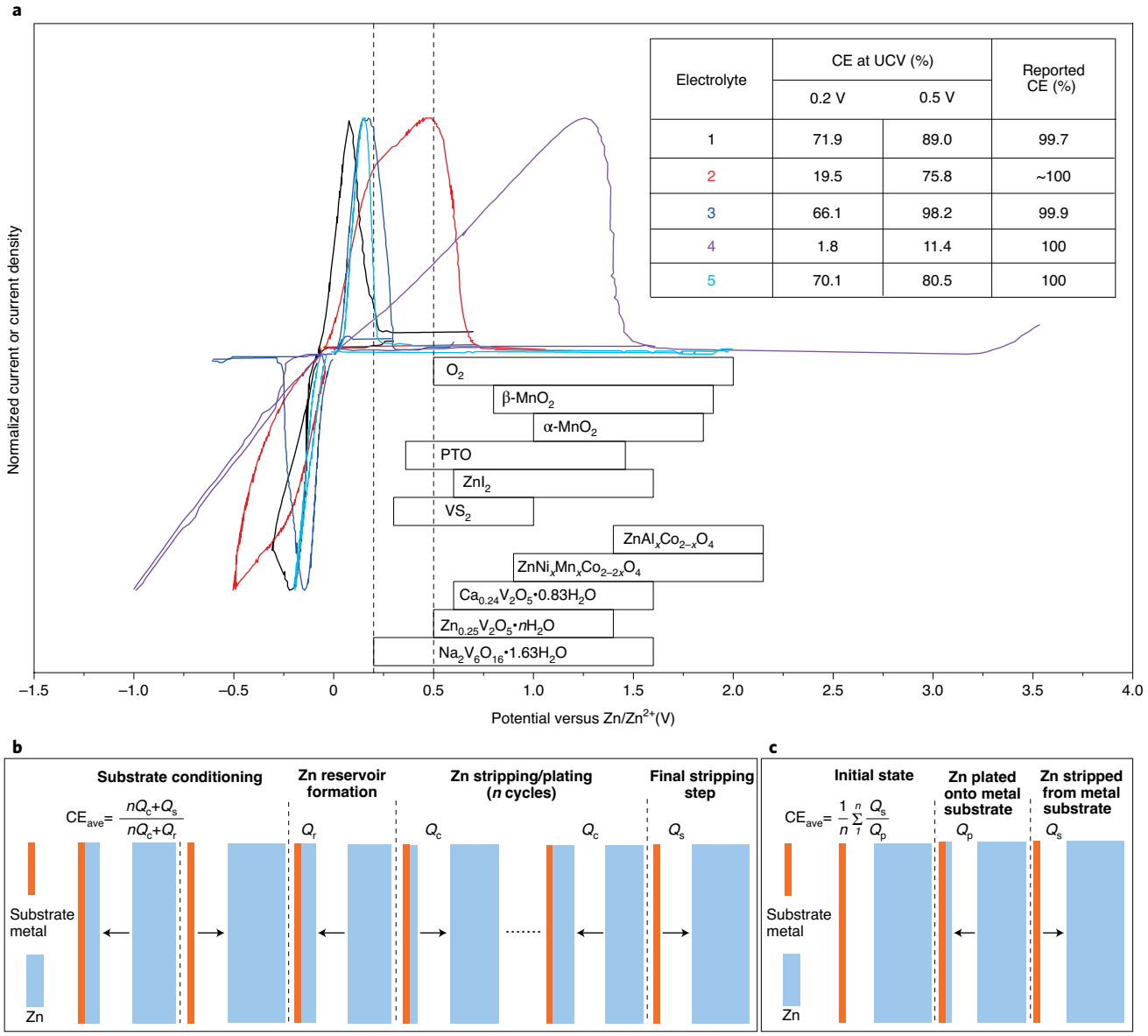

Electrolyte	CE at UCV (%)		Reported CE (%)
	0.2 V	0.5 V	
1	71.9	89.0	99.7
2	19.5	75.8	~100
3	66.1	98.2	99.9
4	1.8	11.4	100
5	70.1	80.5	100

Fig. 2 | CV and galvanostatic methods for CE determination. a, A summary of published CV curves for CE determination in selected Zn electrolytes: 1, $Zn(OTf)_2$/LiTFSI/acetamide (10/20/70 by mol)[23]; 2, $Zn(TFSI)_2$/acetamide (1/7 by mol)[24]; 3, 1 m $Zn(TFSI)_2$ + 20 m LiTFSI in H_2O (ref. [6]); 4, 0.5 M $Zn(TFSI)_2$ in propylene carbonate[22]; 5. 1 M $Zn(OTf)_2$ in H_2O (ref. [19]); compared with the operating potential ranges (floating bars) of different Zn cathode chemistries under development[4–6,11,15,21,45–49]. PTO, pyrene-4,5,9,10-tetraone. The current or current density is normalized to compare scan windows. The table of values in the top right shows reported CE values versus values calculated via integration with more realistic upper cut-off voltages (UCVs, 0.2 V and 0.5 V). The original integration plots are available from the corresponding authors upon reasonable request. **b**, A schematic of the proposed 'reservoir half-cell' galvanostatic protocol[29] for screening Zn plating/stripping CEs. The substrate is conditioned by plating/stripping a certain amount of Zn, followed by deposition of a Zn reservoir (Q_r). A fixed capacity of Zn (Q_c) is cycled n times before all the removable Zn (Q_s) is stripped. The average CE is then calculated using the equation in the inset. **c**, A schematic of the proposed 'reservoir free' galvanostatic protocol for evaluating Zn stripping/plating CE. A fixed capacity of Zn (Q_p) was plated on the substrate and stripped (Q_s) during each cycle. Average CE of n cycles is calculated using the equation in the inset. Panel **b** adapted with permission from ref. [29], Wiley.

Increasing deposition time by a factor of ten, however, leads to the eventual growth of platelets at these accelerated rates (compare Fig. 3f and Fig. 3k). Here an often-overlooked issue of how battery reversibility depends on rates merits particular attention. While these efficiency improvements at high rate are attractive for fast charge and discharge applications (Fig. 3a), the actual battery operation lifetime might not be as impressive as implied by the apparent cycle numbers, particularly if it is cycled at low rates or left at a high state of charge as suggested by Dahn and co-workers[31].

However, the total capacity of Zn that can be plated before a short circuit occurs scales inversely with the plated capacity per cycle in this $ZnSO_4$ system (Fig. 3h), indicating that achieving high DOD with thick Zn films is still challenging despite high apparent CE values. In fact, DOD is an important metric for determining how much of the promised high energy density can be realized at the device level[32]. At the same plated capacity per cycle (only 1 mAh cm^{-2} in this case), the cycle life of Zn anodes substantially increases with increasing current (Fig. 3a) due to the denser Zn deposition achieved at high rate. On the basis of this rate dependence of Zn

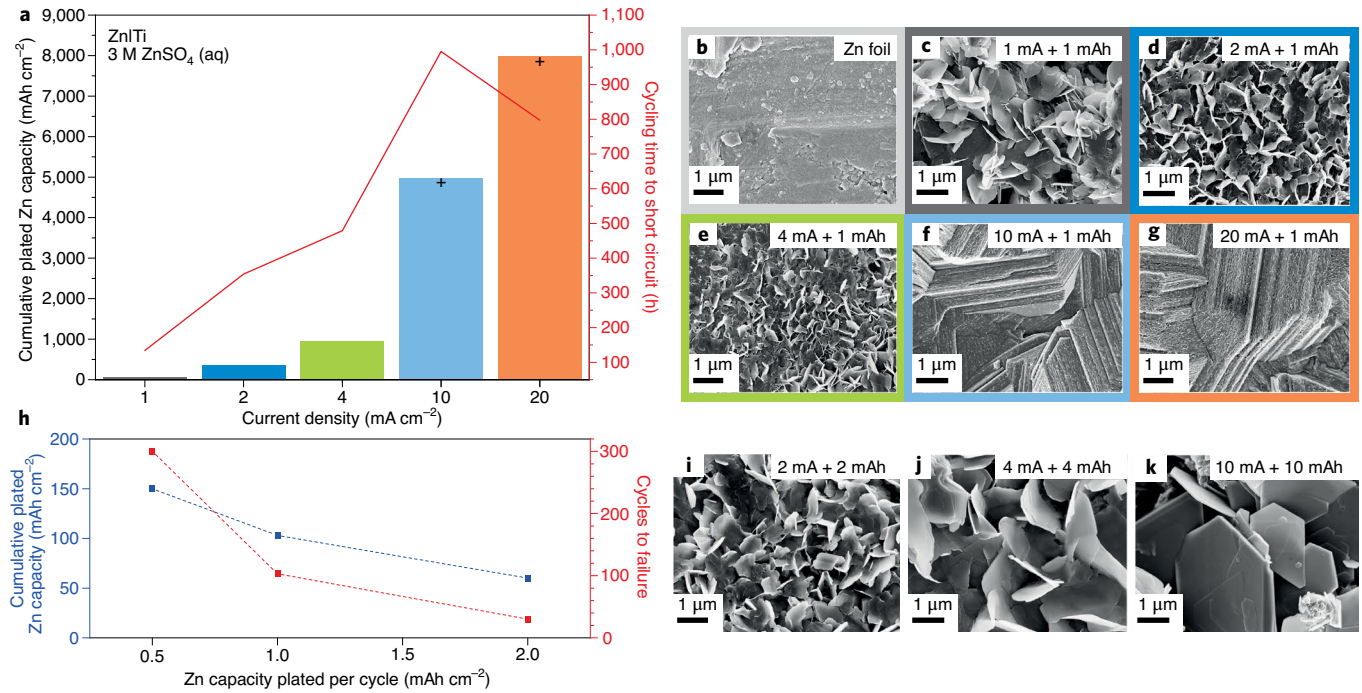

Fig. 3 | Connecting current density and areal capacity to cumulative plated Zn capacity, morphology and cycle life. a, Cycling duration to a short circuit as a function of current density in Zn|Ti cells with 3 M $ZnSO_4$ electrolyte at the same capacity per cycle (1 mAh cm^{-2}), the '+' signs above the 10 and 20 mA cycle life columns indicate that the cycling continues further. **b**–**g**,**i**–**k**, SEM images showing morphology of the pristine Zn electrode before cycling (**b**) and after cycling under the conditions as noted in the figures (note all current densities and areal capacities are given on a per 1 cm^2 basis): 1 mA and 1 mAh (**c**); 2 mA and 1 mAh (**d**); 4 mA and 1 mAh (**e**); 10 mA and 1 mAh (**f**); 20 mA and 1 mAh (**g**); 2 mA and 2 mAh (**i**); 4 mA and 4 mAh (**j**); 10 mA and 10 mAh (**k**). **h**, Total Zn capacity plated on Ti before short circuit as a function of areal capacity per cycle. Panels **a**,**b**–**g**,**i**–**k** reproduced with permission from ref. [34], American Chemical Society.

Table 1 | A summary of selected key factors that could limit Zn reversibility and approaches proposed in the literature to address them for both aqueous and non-aqueous electrolytes

Electrolyte	Key factors	Relevant approaches
Aqueous electrolyte	pH dependent challenges (for example, hydrogen evolution, ZnO formation)	Additives/supporting salts[6,17] Artificial interphases[38,39] Novel Zn architectures[18,36,37]
Non-aqueous electrolyte	Solvent–ZnO reactivity Solvation strength Viscosity	Solvents with high free solvation energy[14,21,29] Solvents reacting with ZnO to form 'dendrite free' solid–electrolyte interphase[14,29] Eutectic ionic liquid[24,43] Hybrid with water[41]

morphology, a protocol of variable rate could bring tangible benefits: an initial fast deposition at high current pulse, followed by relaxation of the salt concentration polarization near the Zn anode after each shallow high current charge pulse. Such a protocol leads to high-quality Zn deposition of low porosity and non-dendritic Zn morphology, as evidenced by the prolonged cycle life in both acidic and alkaline aqueous Zn electrolytes[33,34].

A reversal of the above rate dependence occurs when the electrolyte solution is super-concentrated, in which non-dendritic Zn deposition is favoured by low current density of plating, as suggested by Fig. 1b in ref. [6]. This water-in-bisalt (20 m LiTFSI + 1 m $Zn(TFSI)_2$) electrolyte yielded dense Zn deposition even during cycling at a low current density (0.2 mA cm^{-2})[6]. The exclusion of water from the Zn solvation sheath by a super-concentrated Li supporting salt suppressed water decomposition and formation of Zn hydroxide/oxide. However, this electrolyte does not support high charging rates due to high viscosity and low Zn contribution to the overall conductivity[6,34]. Thus, it is critical to screen the reversibility of promising new Zn material systems at various current densities, DOD and cycle lifetimes to establish a full understanding of the strengths and limitations of a particular system, as well as its commercial viability.

Improving Zn reversibility

A standard protocol for CE determination and knowledge of the key factors dictating Zn reversibility will enable further improvements in Zn metal battery performance. As aqueous and non-aqueous electrolytes differ substantially in both bulk and interfacial structures, specific strategies are needed to improve performance of each class, as summarized in Table 1.

Aqueous Zn electrolytes can be classified based on their pH, which affects the Zn species in the electrolyte as shown in a Pourbaix diagram. In alkaline systems, once hydroxyzincates reach saturation, zinc oxide (ZnO) forms and deposits on the Zn surface. It has been reported that the Zn distribution is not uniform, and instead forms toroidal crystals with metallic zinc surrounded by ZnO (ref. [35]). The presence of ZnO is ambivalent: it protects Zn from corrosion and

leads to an exceptionally low self-discharge rate of 0.8 ± 0.4% yr^{-1} (ref. [36]), but also leads to low CEs and dendrite formation in traditional alkaline electrolytes (for example, 6 M KOH)[6,18]. Advanced architectures such as three-dimensional Zn sponge anodes[37] and a backside-plating configuration[18] mitigate dendrite growth issues and optimize the ZnO to Zn ratio. Neutral or mildly acidic electrolytes (for example, $ZnSO_4$, $Zn(OTf)_2$)[6,17,19,38] do not form passivating Zn oxides/hydroxides on the surface according to the Pourbaix diagram. However, the mildly acidic environment corrodes Zn, which adversely affects Zn plating/stripping CE and promotes dendrite propagation. Diverse strategies have been exercised to stabilize Zn under these conditions, including artificial passivation layers (for example, zirconium dioxide, polyamide)[38,39], or the doping of certain metals (for example, bismuth[40]).

Another often-overlooked issue that may mislead one in evaluating Zn reversibility is the creation of 'soft shorts' that Albertus et al. once highlighted for the Li metal anode[25]. Such a phenomenon, common to all metal batteries and particularly under aggressive performance conditions such as high plating current, can be rather elusive to detect. One possible example can be found in an effort to protect the Zn surface with a polyamide coating (Fig. 5b in ref. [38]), where a rectangular voltage profile (indicating no concentration polarization) and much smaller overpotential occur although the current density has been increased by a factor of 20. These observations suggest that this specific cell possibly formed a soft short in its first cycle, as indicated by the spike at the very initial plating process. The high Zn reversibility demonstrated after the soft short is thus questionable, although the benign effect of polyamide on Zn reversibility at low cycling rate is encouraging. Future studies directly exploring the factors contributing to the timescale and propensity for dendrite formation/failure (that is, interelectrode distance, current density, electrolyte chemistry, temperature and so on) will be critical to the ultimate goal of developing a safe, rechargeable Zn battery chemistry.

An alternative approach to improve Zn reversibility is to alter the Zn solvation sheath via addition of supporting salts. This approach can help overcome the poor solubility of Zn salts in water to achieve some of the beneficial effects observed in super-concentrated electrolytes. In one demonstration, this approach enhanced the Zn CE by suppressing the presence of $[Zn(H_2O)_6]^{2+}$ and shifting the solution pH from mildly acidic to neutral[6]. The effect of supporting salts, and in particular the effect of different supporting cations based on onium structures, has recently become a topic of increasing interest[6,41].

Non-aqueous electrolytes constitute another option for RZMBs to circumvent the inherent drawbacks of aqueous systems (for example, hydrogen evolution, corrosion), and Zn^{2+} solvation plays a powerful role in determining the efficiency of Zn electrochemistry. In an analogous metal anode system, a solvating power series was recently established for selecting appropriate solvents to support a highly reversible Li metal anode[42]. Testing this theory on Zn electrolytes, density functional theory calculations were used to predict relative solvating strength of various solvents by computing the bulk solvation free energy of Zn^{2+} via the cluster-continuum approach[29]. The trends in Zn^{2+} solvation strength were compared against CEs tested using the above-proposed galvanostatic protocol, revealing a similar intrinsic relationship[29]. This correlation between solvation free energy and CE can serve as a guide for future efforts in designing non-aqueous Zn electrolytes. Another critical finding was that solvent reactivity with ZnO is an important factor in understanding solid–electrolyte interphase formation, interfacial impedance growth and dendrite prevention[29]. Eutectic ionic liquids have also achieved CE improvements by modifying the interface[24,43]. To address conductivity and viscosity issues in eutectic ionic liquids, a trace amount of water can function as a 'lubricant' for uniform Zn deposition without compromising electrochemical performance[41]. Such efforts obscure the once clear demarcation between aqueous and non-aqueous electrolytes, resulting in hybrid electrolytes that may combine the merits of both classes.

Outlook

CE is the most important parameter for rapidly benchmarking the efficiency of a battery's chemistry, but its reliability as a universal descriptor depends on the field's adoption of a consistent methodology with conditions relevant to the intended applications. In this Perspective, we revealed the considerable gap between reported CE results and their relevance for practical RZMBs. For Zn, or perhaps all metal-based battery chemistries, CV should be excluded as a method for CE determination in future studies besides its role as a preliminary screening technique. Instead, we propose a galvanostatic reservoir CE protocol with standard parameters for current density, areal capacity and upper cut-off voltage as a powerful screening tool for gauging commercial viability of Zn systems and establishing a better understanding of the links between plating/stripping reversibility and Zn morphology, dendrite formation and cycle life. To start approaching competitive energy densities in commercially realistic cell formats, the use of thinner Zn foil (≤30 μm) cycled to higher DODs with a limited volume of electrolyte is encouraged in future measurements performed with ultrahigh precision testing equipment[44]. We hope that this Perspective will provide useful guidelines to the ongoing development of novel Zn cathode materials, so that advances in each RZMB component can be synchronized to maintain an understanding of practically achievable full cell performance.

Methods

Calculation of key parameters. Figure 1 shows a summary of the representative Zn plating/stripping CE values in the literature and the relevant parameters selected for those measurements. These parameters are important for developing batteries leveraging a practical Zn metal anode.

In galvanostatic studies, the current density was usually provided in the literature, but for CV studies, we calculated an effective current density for comparison. To do this, we integrated the area below 0 V (versus Zn/Zn^{2+}) in digitized CV plots from published studies. The total integrated area was then divided by the potential range to obtain the average current. Finally, the average current was divided by the area of working electrode to obtain the average current density.

Areal capacity plated per cycle was also explicitly provided in galvanostatic studies. For CV, an areal capacity plated per cycle was approximated by multiplying the average current density by the duration of the CV scan in the plating window.

The areal capacity per micrometre (an area of 1 cm^2) is calculated by the following equation.

$$\text{Areal capacity per micrometre} = 2 \times \text{Mole number of Zn per micrometre} \times \text{Faraday constant} \quad (1)$$

Then the thickness of Zn passed per cycle is calculated by using areal capacity plated per cycle over capacity per micrometre (0.586 mAh $(cm^2 \times \mu m)^{-1}$). The fraction of Zn passes per cycle is calculated by using the thickness of Zn passed per cycle over the total thickness of Zn electrode.

Cumulative capacity plated is calculated by multiplying current density by the total time of Zn plating based on Zn|Zn or Zn|substrate metal cell cycling results reported in the literature.

Data availability

The datasets analysed and generated during this study are included in the paper and its Supplementary Information.

Received: 17 April 2020; Accepted: 14 July 2020;
Published online: 14 August 2020

References

1. Pillot, C. *Worldwide Rechargeable Battery Market 2019-2030* (Avicenne Energy, 2020).
2. Tahil, W. *The Trouble With Lithium* (Meridian International Research, 2007); http://go.nature.com/jhDqLH
3. Turcheniuk, K., Bondarev, D., Singhal, V. & Yushin, G. Ten years left to redesign lithium-ion batteries. *Nature* **559**, 467–470 (2018).
4. Kundu, D., Adams, B. D., Duffort, V., Vajargah, S. H. & Nazar, L. F. A high-capacity and long-life aqueous rechargeable zinc battery using a metal oxide intercalation cathode. *Nat. Energy* **1**, 16119 (2016).
5. Pan, H. et al. Reversible aqueous zinc/manganese oxide energy storage from conversion reactions. *Nat. Energy* **1**, 16039 (2016).

6. Wang, F. et al. Highly reversible zinc metal anode for aqueous batteries. *Nat. Mater.* **17**, 543–549 (2018).
7. Zhang, C. et al. A $ZnCl_2$ water-in-salt electrolyte for a reversible Zn metal anode. *Chem. Commun.* **54**, 14097–14099 (2018).
8. Wang, L. et al. A $Zn(ClO_4)_2$ Electrolyte enabling long-life zinc metal electrodes for rechargeable aqueous zinc batteries. *ACS Appl. Mater. Interfaces* **11**, 42000–42005 (2019).
9. Winter, M., Barnett, B. & Xu, K. Before Li ion batteries. *Chem. Rev.* **118**, 11433–11456 (2018).
10. Yaroshevsky, A. A. Abundances of chemical elements in the Earth's crust. *Geochem. Int.* **44**, 48–55 (2006).
11. Zhang, N. et al. Rechargeable aqueous zinc-manganese dioxide batteries with high energy and power densities. *Nat. Commun.* **8**, 405 (2017).
12. Wang, D. et al. A zinc battery with ultra-flat discharge plateau through phase transition mechanism. *Nano Energy* **71**, 104583 (2020).
13. He, P. et al. Layered VS_2 nanosheet-based aqueous Zn ion battery cathode. *Adv. Energy Mater.* **7**, 1601920 (2017).
14. Naveed, A., Yang, H., Yang, J., Nuli, Y. & Wang, J. Highly reversible and rechargeable safe Zn batteries based on a triethyl phosphate electrolyte. *Angew. Chem. Int. Ed.* **58**, 2760–2764 (2019).
15. Guo, Z. et al. An environmentally friendly and flexible aqueous zinc battery using an organic cathode. *Angew. Chem. Int. Ed.* **57**, 11737–11741 (2018).
16. Zhao, J. et al. "Water-in-deep eutectic solvent" electrolytes enable zinc metal anodes for rechargeable aqueous batteries. *Nano Energy* **57**, 625–634 (2019).
17. Huang, J. et al. Thickening and homogenizing aqueous electrolyte towards highly efficient and stable Zn metal batteries. *J. Electrochem. Soc.* **166**, A1211–A1216 (2019).
18. Higashi, S., Lee, S. W., Lee, J. S., Takechi, K. & Cui, Y. Avoiding short circuits from zinc metal dendrites in anode by backside-plating configuration. *Nat. Commun.* **7**, 11801 (2016).
19. Zhang, N. et al. Cation-deficient spinel $ZnMn_2O_4$ cathode in $Zn(CF_3SO_3)_2$ electrolyte for rechargeable aqueous Zn-ion battery. *J. Am. Chem. Soc.* **138**, 12894–12901 (2016).
20. Zhang, N. et al. Ultrafast rechargeable zinc battery based on high-voltage graphite cathode and stable nonaqueous electrolyte. *ACS Appl. Mater. Interfaces* **11**, 32978–32986 (2019).
21. Naveed, A. et al. A highly reversible Zn anode with intrinsically safe organic electrolyte for long-cycle-life batteries. *Adv. Mater.* **31**, 1900668 (2019).
22. Han, S. D. et al. Origin of electrochemical, structural, and transport properties in nonaqueous zinc electrolytes. *ACS Appl. Mater. Interfaces* **8**, 3021–3031 (2016).
23. Zhang, J. et al. Amide-based molten electrolyte with hybrid active ions for rechargeable Zn batteries. *Electrochim. Acta* **280**, 108–113 (2018).
24. Qiu, H. et al. Zinc anode-compatible in-situ solid electrolyte interphase via cation solvation modulation. *Nat. Commun.* **10**, 5374 (2019).
25. Albertus, P., Babinec, S., Litzelman, S. & Newman, A. Status and challenges in enabling the lithium metal electrode for high-energy and low-cost rechargeable batteries. *Nat. Energy* **3**, 16–21 (2018).
26. Albertus, P. Integration and optimization of novel ion-conducting solids (IONICS). *Advanced Research Projects Agency* https://arpa-e.energy.gov/?q=arpa-e-programs/ionics (2016).
27. Bard, A. J. & Faulkner, L. R. *Electrochemical Methods: Fundamentals and Applications* (Wiley, 2001).
28. Adams, B. D., Zheng, J., Ren, X., Xu, W. & Zhang, J.-G. Accurate determination of coulombic efficiency for lithium metal anodes and lithium metal batteries. *Adv. Energy Mater.* **8**, 1702097 (2018).
29. Ma, L. et al. Critical factors dictating reversibility of the zinc metal anode. *Energy Environ. Mater.* https://doi.org/10.1002/eem2.12077 (2020).
30. Aurbach, D. & Gofer, Y. The behavior of lithium electrodes in mixtures of alkyl carbonates and ethers. *J. Electrochem. Soc.* **138**, 3529–3536 (1991).
31. Burns, J. C. et al. Evaluation of effects of additives in wound Li-ion cells through high precision coulometry. *J. Electrochem. Soc.* **158**, A255–A261 (2011).
32. Parker, J. F., Ko, J. S., Rolison, D. R. & Long, J. W. Translating materials-level performance into device-relevant metrics for zinc-based batteries. *Joule* **2**, 2519–2527 (2018).
33. Garcia, G., Ventosa, E. & Schuhmann, W. Complete prevention of dendrite formation in Zn metal anodes by means of pulsed charging protocols. *ACS Appl. Mater. Interfaces* **9**, 18691–18698 (2017).
34. Glatz, H., Tervoort, E. & Kundu, D. Unveiling critical insight into the Zn metal anode cyclability in mildly acidic aqueous electrolytes: implications for aqueous zinc batteries. *ACS Appl. Mater. Interfaces* **12**, 3522–3530 (2020).
35. Nakata, A. et al. In situ Zn/ZnO mapping elucidating for "shape change" of zinc electrode. *APL Mater.* **6**, 047703 (2018).
36. Hopkins, B. J. et al. Fabricating architected zinc electrodes with unprecedented volumetric capacity in rechargeable alkaline cells. *Energy Storage Mater.* **27**, 370–376 (2020).
37. Parker, J. F. et al. Rechargeable nickel-3D zinc batteries: an energy-dense, safer alternative to lithium-ion. *Science* **356**, 415–418 (2017).
38. Zhao, Z. et al. Long-life and deeply rechargeable aqueous Zn anodes enabled by a multifunctional brightener-inspired interphase. *Energy Environ. Sci.* **12**, 1938–1949 (2019).
39. Liang, P. et al. Highly reversible Zn anode enabled by controllable formation of nucleation sites for Zn-based batteries. *Adv. Funct. Mater.* **30**, 1908528 (2020).
40. Park, J. H. et al. Control of growth front evolution by bi additives during ZnAu electrodeposition. *Nano Lett.* **18**, 1093–1098 (2018).
41. Bayer, M. et al. Influence of water content on the surface morphology of zinc deposited from EMImOTf/water mixtures. *J. Electrochem. Soc.* **166**, A909–A914 (2019).
42. Su, C. C. et al. Solvating power series of electrolyte solvents for lithium batteries. *Energy Environ. Sci.* **12**, 1249–1254 (2019).
43. Ma, L. et al. Hydrogen-free and dendrite-free all-solid-state Zn-ion batteries. *Adv. Mater.* **32**, 1908121 (2020).
44. Smith, A. J., Burns, J. C., Trussler, S. & Dahn, J. R. Precision measurements of the Coulombic efficiency of lithium-ion batteries and of electrode materials for lithium-ion batteries. *J. Electrochem. Soc.* **157**, A196–A202 (2010).
45. Pan, C., Nuzzo, R. G. & Gewirth, A. A. $ZnAl_xCo_{2-x}O_4$ spinels as cathode materials for non-aqueous Zn batteries with an open circuit voltage of ≤2 V. *Chem. Mater.* **29**, 9351–9359 (2017).
46. Pan, H. et al. Controlling solid–liquid conversion reactions for a highly reversible aqueous zinc–iodine battery. *ACS Energy Lett.* **2**, 2674–2680 (2017).
47. Xia, C., Guo, J., Li, P., Zhang, X. & Alshareef, H. N. Highly stable aqueous zinc-ion storage using a layered calcium vanadium oxide bronze cathode. *Angew. Chem. Int. Ed.* **57**, 3943–3948 (2018).
48. Hu, P. et al. Highly Durable $Na_2V_6O_{16}{\cdot}1.63H_2O$ nanowire cathode for aqueous zinc-ion battery. *Nano Lett.* **18**, 1758–1763 (2018).
49. Pan, C., Zhang, R., Nuzzo, R. G. & Gewirth, A. A. $ZnNi_xMn_xCo_{2-2x}O_4$ spinel as a high-voltage and high-capacity cathode material for nonaqueous Zn-ion batteries. *Adv. Energy Mater.* **8**, 1800589 (2018).

Acknowledgements

This work was supported by the Joint Center for Energy Storage Research (JCESR), an Energy Innovation Hub funded by Department of Energy, through IAA SN2020957. L.M. also acknowledges the Army Research Laboratory for providing financial support under the Dr. Brad. E. Forch Distinguished Postdoctoral Fellowship administered by the National Research Council. We thank P. Albertus (UMD) for useful discussions.

Competing interests

The authors declare no competing interests.

Additional information

is available for this paper at https://doi.org/10.1038/s41560-020-0674-x.

Correspondence should be addressed to M.A.S. or K.X.